Journal of Orthopaedic Translation (2015) 3, 134—141

Available online at www.sciencedirect.com

ScienceDirect

journal homepage: http://ees.elsevier.com/jot

ORIGINAL ARTICLE

In vivo three-dimensional magnetic resonance imaging of rat knee osteoarthritis model induced using meniscal transection

Yi-Xiang J. Wang [a,*], Junqing Wang [a], Min Deng [a], Gang Liu [b], Ling Qin [c]

[a] *Department of Imaging and Interventional Radiology, Faculty of Medicine, The Chinese University of Hong Kong, Prince of Wales Hospital, Shatin, New Territories, Hong Kong SAR, China*
[b] *Centre for Molecular Imaging and Translational Medicine, School of Public Health, Xiamen University, Xiamen, China*
[c] *Department of Orthopaedics and Traumatology, Faculty of Medicine, The Chinese University of Hong Kong, Prince of Wales Hospital, Shatin, New Territories, Hong Kong SAR, China*

Received 23 May 2015; received in revised form 2 June 2015; accepted 4 June 2015
Available online 23 June 2015

KEYWORDS
animal model;
articular cartilage;
femorotibial joint;
osteoarthritis;
subchondral bone

Summary *Background/Objective:* In a rat meniscal tear model of osteoarthritis (OA), a full-thickness cut in the medial meniscus leads to joint instability and progressive development of knee OA. This study evaluated *in vivo* high-resolution three-dimensional magnetic resonance imaging (3D MRI) in demonstrating the knee joint structural changes of this animal model.
Methods: A left knee meniscal tear procedure was carried out on 10 rats, and sham surgery was performed on five rats. The joints were MRI scanned 44 days after surgery at 4.7 Tesla. A 3D data set was acquired using a 3D spoiled gradient echo sequence at a resolution of $59 \times 117 \times 234\ \mu m^3$. After MRI, microscopic examination of the joints was performed.
Results: The medial meniscus tear was clearly visible with MRI. Cartilage damage was seen in all animals, with varying degrees of severities, which included a decrease of cartilage thickness and loss of cartilage in some areas, and focal neocartilage proliferation at the joint margin. Damage to the subchondral bone included local osteosclerosis, deformed tibia cortex surface, and osteophytes. The damage to the cartilage and bone was most extensive on the weight-bearing region of the medial tibial plateau. No apparent subchondral bone damage was observed in the epiphysis of the femur. In five animals, single or multiple high MR signal areas were seen within the epiphysis of the tibia, consistent with epiphyseal cyst formation. The knee interarticular space on the media side was slightly increased in two animals. Mild femur—tibia axis misalignment was seen in one animal. Changes seen on MRI were consistent with histopathological changes.

* Corresponding author. Department of Imaging and Interventional Radiology, Faculty of Medicine, The Chinese University of Hong Kong, Prince of Wales Hospital, Shatin, New Territories, Hong Kong SAR, China.
E-mail address: yixiang_wang@cuhk.edu.hk (Y.-X.J. Wang).

http://dx.doi.org/10.1016/j.jot.2015.06.002

Conclusion: MRI offers *in vivo* information on the pathogenesis change of rat knee OA induced with menisectomy. It can serve as a supplement technique to histology, as it is particularly useful for longitudinal follow-up of OA model development.

Introduction

Osteoarthritis (OA) is a degenerative joint disease that affects a large and growing population. It is a progressive disorder of the joints caused by a gradual loss of hyaline cartilage resulting in the development of bony spurs and cysts at the margins of the joints, and has a complex pathology characterised by biochemical and enzymatic changes, cartilage damage (fibrillation and erosion), and bone remodelling (osteophyte formation and bone sclerosis). Advances in medical imaging, and especially magnetic resonance imaging (MRI), offer early diagnosis and therapeutic follow-up both in clinics and in animal models of OA. Animal models of arthritis are widely used preclinically to investigate the pathogenesis mechanism of degenerative OA, as well as to evaluate potential antiarthritis drugs for clinical use. Many experimental models of rat OA have been developed, and their histological and biochemical characteristics are established [1—3].

In general, OA animal models are divided into two main categories: spontaneous joint degeneration models and experimentally induced OA models; the latter category is further subdivided into biochemically induced OA and biomechanically induced OA. Biochemical induction is achieved with intra-articular injection of proteolytic agents that induce lysis of specific cartilage constituents, such as collagen, proteoglycans, and/or chondrocytes. Biomechanical induction, however, involves the initiation of biomechanical instability through surgical transection of a ligament or the meniscus, or a combination of both. Animal models of biomechanically induced OA include anterior cruciate ligament transection in dogs, lateral meniscectomy in sheep, partial meniscectomy in rabbits, meniscectomy in guinea pigs and rats, and cruciate ligament transection in rats [1—8]. High resolution MRI can noninvasively demonstrate the detailed anatomy and pathological changes, including progression and regression of joint changes of bone, cartilage, synovium, fascia, muscles, and other soft tissues [9—13]. MRI has also been used to assess therapeutic effects in animal models, allowing paired comparisons, and increasing statistical power of experiments, and reducing the amount of animal usage [14—16]. Increasingly, the resolution of high magnetic strength MR scanners reaches close to histology level [17—19]. Goebel et al [20] reported good reproducibility for normal rat femorotibial cartilage volume assessment using 7T MRI. Huang et al [21] investigated the treatment effect of hyaluronic acid on cartilage in OA by measuring the MR T2 value of cartilage in an anterior cruciate ligament transection rat OA model.

The menisci plays an important role in load-bearing distribution at the knee. Clinically, loss of meniscal function due to meniscal extrusion and meniscectomy result in increased mechanical loading of the articular cartilage and subchondral bone of the affected knee [22,23]. Total meniscectomy increases the risk of initiation and progression of knee OA radiographically by 14-fold after 21 years [24]. In the rat meniscal tear model of OA, a full-thickness cut in the medial meniscus, and in some studies plus transection of the medial collateral ligament, leads to joint instability and progressive development of OA characterised by proteoglycan loss, cartilage fibrillation, chondrocyte death, eventual damage to the subchondral bone, and formation of osteophytes [1—3]. Rat knee OA induced with meniscal transection offers the advantages of site specificity, known time to disease onset, and a relatively short development time [1,2]. The cartilage lesions that occur in the rat meniscal tear model are morphologically similar to those that occur in human OA but occur much more rapidly. This may be due to the rats normally using their unstable joint immediately after surgery whereas humans and other animals such as dogs do not immediately load their knee joint after surgery. Rats have very little spontaneous degeneration in their knee joints, so lesions observed are generally a result of surgical manipulation only [5]. It was reported that lesions were reasonably consistent if the surgical technique is consistent [1]. The current study aimed to evaluate *in vivo* high-resolution three-dimensional (3D) MRI in demonstrating joint structural changes in the meniscal tear model of OA in rats.

Materials and methods

All *in vivo* procedures were approved by the local Animal Experimentation Ethics Committee. Fifteen Han Wistar male rats, breed at Xiamen University, China, were aged 11—12 weeks when the studies were initiated. This animal age was similar to those in the literature reports [1,25,26]. Two to three animals were housed per stainless steel cage on a 12-hour light/12-hour dark cycle in an air-conditioned room at 22°C, and were checked daily by the animal care staff. A standard commercial rat chow (Prolab RMH 2500, PMI Nutrition International LLC, Brentwood, USA) and water were available *ad libitum*. The animals were thoroughly examined immediately after arrival and subsequently underwent a thorough daily clinical examination which included body weight, physical condition, and behaviour.

Rats were anesthetized by using a combination of xylazine 10 mg/kg body weight and ketamine 90 mg/kg. The operation was carried out by a staff member experienced in animal surgery. The left leg of the rat was shaved and the

skin cleaned with suitable skin antiseptic. With the leg held in an extended position a medial parapatellar incision (approximately 5 mm) and arthrotomy were performed. The patella was dislocated laterally and the knee joint fully flexed exposing the medial collateral ligament. An incision was then made anterior to the medial collateral ligament to separate the synovial tissues. Approximately 3 mm of the medial meniscus was freed from its attachments to the margin of the medial tibial plateau. The meniscus was then grasped with fine tipped haemostatic forceps, retracted, and transected with a fine-tipped scissors ($n = 10$ rats). When released, the anterior half of the meniscus retracts anteriorly and the posterior half retracts posteriorly. The incision was closed with a wound closure clip. Sham-operated animals ($n = 5$ rats) were treated identically, except that transection of the meniscus was omitted.

An MR scan was carried out on the 15 animals 44 days after surgery. At this time, the arthritic damage to the joint is known to be apparent [3,16]. Animals were anaesthetised. The MR scanner was a 4.7 Tesla horizontal magnetic resonance system equipped with a 300 mT/m gradient (Agilent/Varian, Palo Alto, California, USA). To increase the signal receiving sensitivity, a special coil was built in-house to fit with the size of rat leg at the level of the knee joint. The radio frequency coil was a double balanced matched 3 cm diameter copper sheet solenoid and was 1 cm in length. A 3D data set was acquired using a spoiled multi-echo fat-suppressed 3D gradient echo (TR = 75 ms, TE = 2.8 ms, flip angle = 30). Scan duration was approximately 50 minutes. The MRI parameters were optimised to allow reasonable scan duration (50 minutes) and best tissue contrast and spatial resolution. Prior to the acquisition of the 3D data set, the overall positioning of the rat was verified using a fast multislice sagittal gradient echo image to ensure that the leg was placed adequately within the radiofrequency coil. Then, a transverse image of the knee was used to select the orientation of the sagittal view of the 3D images such that they were parallel to the medial condyle. Fat suppression in the centre of the coil was achieved using an 8.2 ms Gaussian pulse placed 650 Hz off-resonance from the water signal. The images covered the entire knee joint with a resolution of $59 \times 117 \times 234\ \mu m^3$. Image reconstruction was performed using in-house software developed in Matlab (The Mathworks, Natick, MA, USA).

Following MRI, the animals were scarified for histology. The soft tissue was removed from each leg and the femorotibial joints were isolated by cutting the mid femur and tibia. The intact joints were then preserved in a 10% neutral buffered formalin for 48–72 hours and subsequently decalcified for 24–36 hours in rapid decalcification fluid. Trimmed joint tissues were processed with standard histological techniques and mounted in wax blocks for coronal sectioning. Multiple 4 μm sections at 450 μm steps were prepared through the whole thickness of each block and stained with toluidine blue or haematoxylin and eosin for light microscopy. The MRI data and histology images were analysed on a one animal-to-one animal base by a radiologist and a pathologist experienced in small animal studies.

Results

Three-dimensional high-resolution MR images were obtained in all 15 rats with a high signal-to-noise ratio. The cortical bone and trabeculae and tendon/ligament showed a low signal; menisci showed a low signal intensity with focal intermediate signal; muscle showed an intermediate signal; fat showed a low signal due to the fat suppression technique; cartilage showed a high signal. In one animal, a susceptibility artefact was seen in the surgically operated location. The most likely cause of this artefact was due to the debris of metal surgical instruments remaining in the tissue. This artefact partially affected the assessment of the medial side and the subchondral bone of the tibia of this animal. The medial meniscus tear was clearly visible on MR images, and the five sham-operated animals could be easily identified (Figure 1). It was seen that the anterior

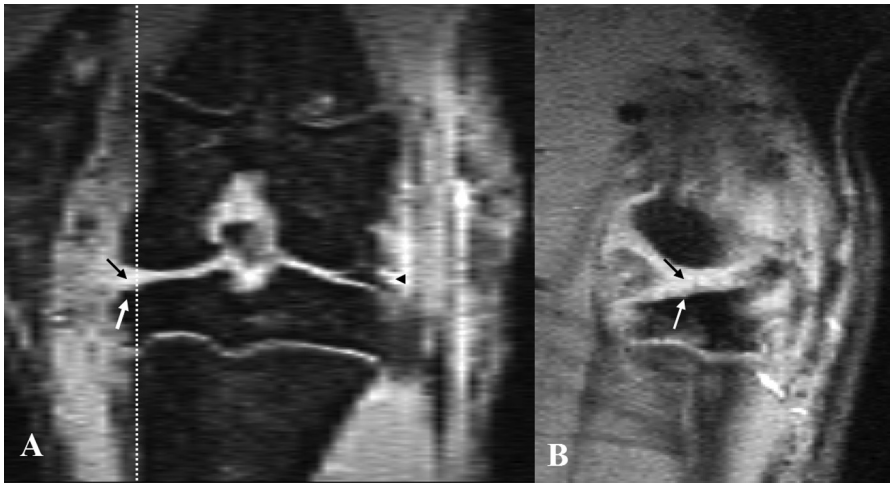

Figure 1 Magnetic resonance imaging of a rat knee with medial meniscal tear: (A) coronal view; (B) sagittal view (corresponding to the level of the dotted line on coronal view). Both images show the media meniscal tear (black arrow). The lateral meniscus is shown to be normal (black arrowhead). Bone damage is also seen (white arrow).

half of the meniscus retracted anteriorly and the posterior half retracted posteriorly. The connective tissue fibrous scar caused by the surgical operation could also be seen on the medial side of the knee joint.

Of the 10 animals with meniscal transection, cartilage damage could also be seen in all animals, with varying degrees of severities. Damage to the cartilage included a decrease of cartilage thickness and loss of cartilage in some areas, and focal neocartilage proliferation at the joint margin (Figure 2). The interface between the bone cortex and cartilage is well defined; however, the interface between the tibia cartilage and intra-articular space is less clear with the current MR technique, therefore the quantification of cartilage loss remained difficult.

Of the nine rats assessed, subchondral bone change can be appreciated in eight animals, again with varying severities. One animal's subchondral bone retained a normal appearance on MRI. Damage to the subchondral bone included local osteosclerosis and deformed tibia cortex surface (Figure 3). Osteophytes also occurred on the medial joint margin of the tibia plateau in some animals (Figure 3). The damage to cartilage and bone was most extensive on the weight-bearing region of the medial tibial plateau. No apparent subchondral bone damage was observed in the epiphysis of the femur. In five animals single or multiple high MR signal areas were seen within the epiphysis of the tibia, consistent with epiphyseal cyst formation (Figure 4). The knee interarticular space on the media side was slightly

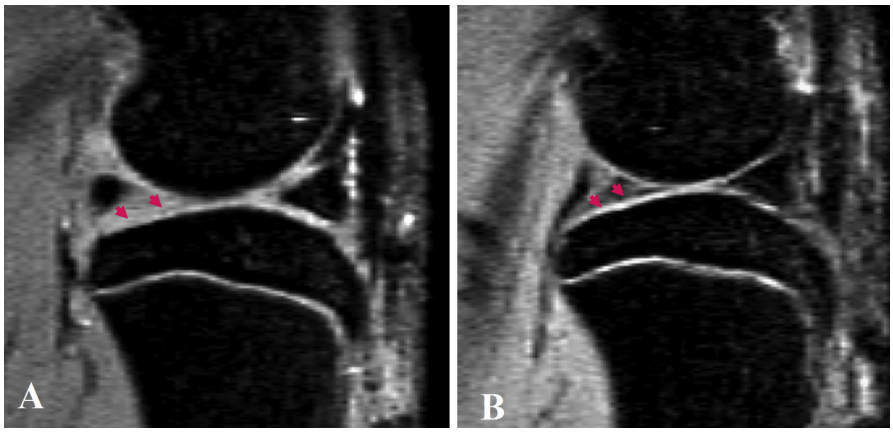

Figure 2 (A) Sagittal view magnetic resonance image of a rat knee with medial meniscal tear. Parts of the tibia cartilage have become much thinner (arrowheads). (B) Sagittal view magnetic resonance image of a rat with sham operation, showing normal tibia cartilage (arrowheads).

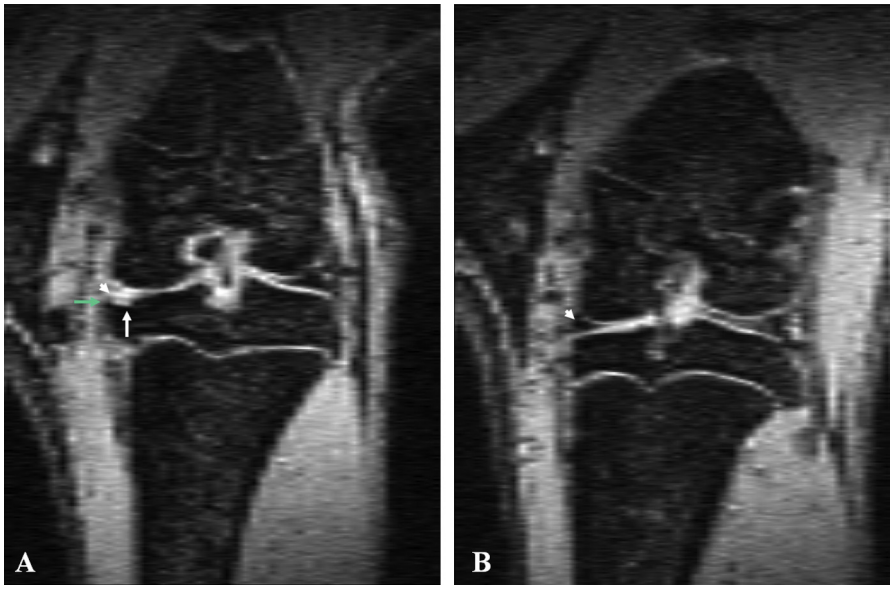

Figure 3 (A) Coronal view magnetic resonance image of a rat knee with medial meniscal tear showing the location of the meniscal tear (white arrowhead), and bone damage at the medial third of the medial tibia plateau (white arrow) and osteophyte (green arrow). (B) Coronal view magnetic resonance image of a rat with sham operation showing the normal meniscus (white arrowhead) and normal tibia plateau.

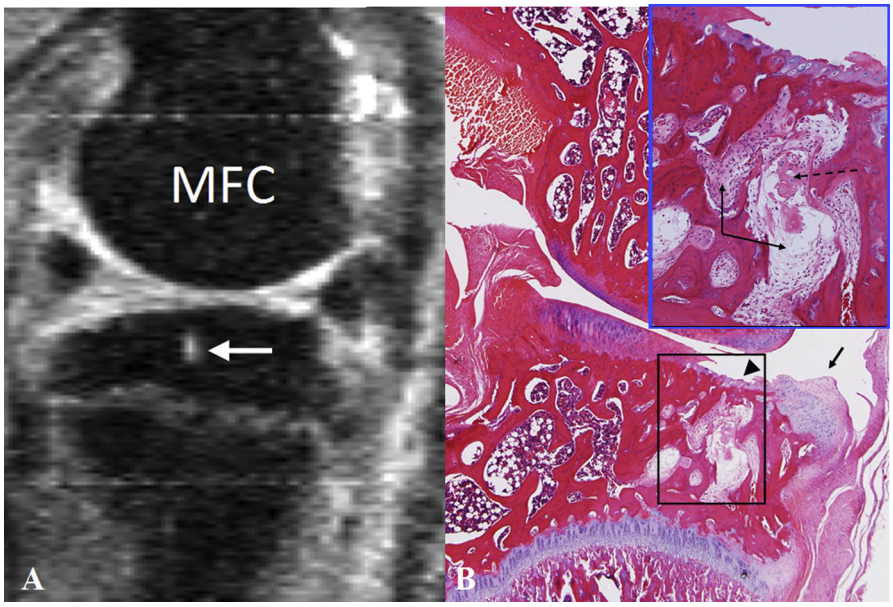

Figure 4 (A) Magnetic resonance image of a rat knee with medial meniscal tear: a cyst is seen in the epiphysis of the tibia (white arrow). (B) Haematoxylin and eosin histology (low power magnification at original magnification × 25, and medium power magnification insert at original magnification × 100) of the medial femorotibial following meniscal transection. The articular cartilage of the tibia shows loss of chondrocytes (arrowhead) and staining pallor reflecting loss of proteoglycan (arrow). There is a vertical fracture in the degenerate cartilage and underlying focal loss of subchondral bone with extrusion of the degenerate matrix through into the marrow space. There is an associated loss of the normal marrow cellularity in the insert region with replacement by cellular infiltrates and fibrous tissue, resulting in epiphyseal cyst formation (insert). MFC = medial femur condyle.

increased in two animals. Mild femur—tibia axis misalignment was seen in one animal. In that animal, the articular capsule was seen bulged outwards toward the media side, suggesting the weakening of ligaments at that side.

Histopathological changes were characterised by a variable severity of cartilage degeneration (Figure 5). There were loss of chondrocytes, and proteoglycan loss evidenced by reduced toluidine blue staining. Fibrillation of the superficial cartilage, vertical, and lateral fractures in the cartilage matrix and ulceration generally to the tide mark were common findings. Notable chondrophytes were present at the lateral borders of both the medial tibial and

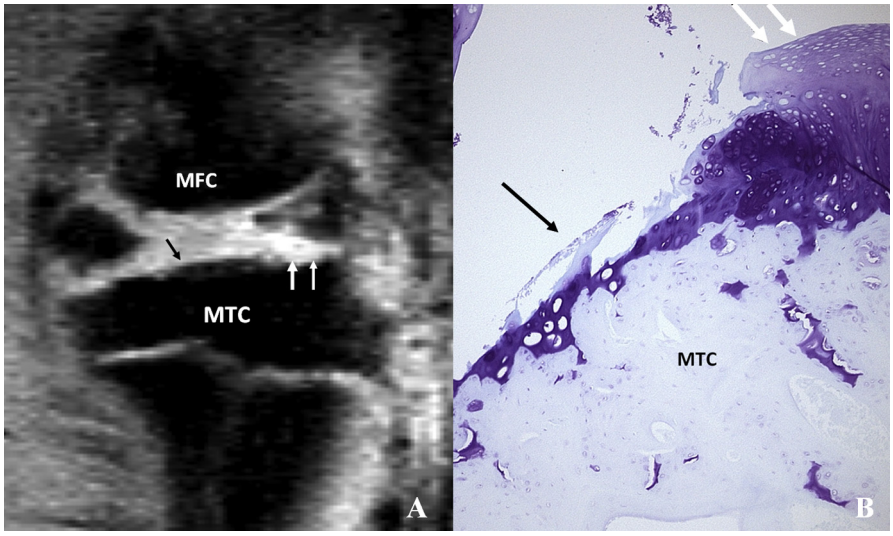

Figure 5 (A) Sagittal view (at peripheral level) magnetic resonance image of a rat knee with medial meniscal tear. Black arrow indicates cartilage thinning, and white arrows indicate neocartilage proliferation. (B) Corresponding coronal histology section of the medial MTC stained with toluidine blue (original magnification x 100) after meniscal tear. Cartilage erosion (arrows) and neocartilage proliferation (dotted arrow) are seen in the tibia cartilage. MFC = media femur condyle; MTC = medial tibia condyle.

femoral condyles. These histopathological changes were generally most severe in the medial tibial cartilage. In some joints further degeneration and destruction of the subchondral bone occurred in areas of cartilage degeneration or ulceration. In these locations extrusion of the degenerate articular cartilage and some bone spicules into the underlying epiphyseal marrow spaces were seen. Within these areas there was a loss of the normal marrow with replacement by cellular infiltrates which included activated osteoclasts, and mononuclear cells including osteoblasts and small to medium sized fibroblast-like cells with fibrous matrix formation. These areas occasionally replaced a substantial proportion of the marrow space and with further degeneration of the cancellous bone of the epiphysis, formed sizable cysts. Occasionally the cystic areas were relatively acellular and contained eosinophilic material, presumably fluid. It was notable that epiphyseal cysts were only present when there was evidence of subchondral bone destruction. These epiphyseal cysts were consistent with the high signal areas seen in the epiphysis of tibia with MRI (Figure 4).

Discussion

In rat knee OA induced using meniscal transection, the loss of meniscal function resulted in cartilage degeneration and subchondral bone defects particularly in the region covered by menisci, which progress over time after surgery [16]. Forty-four days after surgery it was shown that OA changes were well established. Tibial cartilage degeneration was focally severe with degenerative changes of lesser severity in the surrounding matrix and prominent osteophytes [1]. Although it was suggested that lesions were reasonably consistent if the surgical technique is consistent [1], interanimal variability in the response to the meniscal tear was observed, both in our current MRI study and a few literature reports [6,27]. This was probably related to the activity level and joint loading of the individual rats. This OA model enables researchers to quantify cartilage damage during active disease and the action of potential chondroprotective agents, for example, experiments have shown that matrix metalloproteinase inhibition is effective in reducing the joint damage that occurs in this OA model, and fibroblast growth factor-18 can stimulate repair of damaged cartilage [6,27]. With histological assessment, Janusz et al [6] reported that moderate cartilage degeneration of the tibial plateau with focal loss of chondrocytes and proteoglycan loss was observed at Week 1 after meniscal tear and surgical transection of the medial collateral ligament. The cartilage lesions increased slightly in depth and osteophytes were more common at Week 2 with some areas of focally severe cartilage degeneration. Cartilage lesions were often severe by Week 3 with small to large osteophytes. By Week 6 cartilage lesions were often severe and extending beyond a third of the cartilage surface generally seen at Weeks 1–3 and small to large osteophytes were present. The degree of cartilage degeneration of the femur was much less marked than that of the tibial plateau.

Histology remains the gold standard for the assessment of structural change of small OA models. However, histology is limited by its inability to track sequential changes of disease progression in joints, requiring the need to sacrifice groups of animals at specific time points in order to evaluate the disease progression. This approach leads to an inability to assess individual variations among given animals and requires using larger amounts of experimental compounds when the availability of which is often limited. MRI is noninvasive, and can be applied repeatedly to follow the course of structural change development. While histology has superb tissue resolution and contrast, MRI can provide *in vivo* joint information with structures fully intact. It is challenging to study cartilage in rat knee with MRI. By using large animal OA models such as dogs, sheep, and rabbits, the joint anatomical structures will be larger and therefore less demanding on MR spatial resolution. However, these large animal OA models remain expensive and take a significant period of time to develop. Very high resolution and good signal-to-noise ratio are needed to characterise the OA structural changes in rats.

Owing to the fact that bone lacks mobile protons (^{1}H), bone cortex and bone trabeculae have a low signal on MR images, and therefore provide contrast to the surrounding connective tissues such as cartilage, which contains more mobile protons. We used the MR sequence that best delineated the cartilage from the surrounding tissues, i.e., 3D fat-suppressed spoiled gradient echo. However, it should be noted that this sequence is relatively insensitive for bone marrow oedema [12]. In our study with a magnet at 4.7 Tesla field strength, a spatial resolution of $59 \times 117 \times 234$ μm^3 was achieved with a good signal-to-noise ratio. To increase the signal receiving sensitivity, a special coil was built so as to have a tight fit with the rat knee joint, and a shorter echo time of 2.8 ms was selected. Our study showed the anterior half of the meniscus retracted anteriorly and the posterior half retracted posteriorly. Cartilage show high signal and its damage could also be seen in all animals in this study, with varying degree of severities. Femur–tibia axis alignment, and articular capsule, subchondral bone changes, osteophytes are well demonstrated. The interface between bone cortex and cartilage is well defined; however the interface between tibia cartilage and intra-articular space is less clear with the current MR technique, therefore the quantification of cartilage loss remained difficult. Another interesting finding from this study is the cyst formation in tibia epiphysis. Owing to the good tissue contrast, MRI can easily detect these cysts. Pain is the principal symptom of OA [28]. Rat knee OA induced using meniscal transection has been used as an OA pain model [25]. It is well known that cartilage does not contain pain fibres. Bone in the periosteum and bone marrow is richly innervated with nociceptive fibres. In this respect, assessment of bone structure would be more important. Our histology data showed these cysts in the tibia epiphysis were linked to the degree of destruction of the subchondral bone. Since bone marrow is richly innervated with nociceptive fibres, it would be interesting to further investigate the relationship between these cyst formations and pain.

Changes in the femorotibial cartilage are of great interest in studying the structural progression of OA, because changes in thickness can be localized in particular compartments. Additionally, concomitant cartilage erosion,

oedema, and subchondral changes may alter the sensitivity of a global measurement, thus reinforcing the interest of monitoring compartmental changes in cartilage thickness. MRI based 3D evaluation of cartilage thickness has the advantage of being independent of positioning of the knee, whereas histological assessments are made on 2D slices, and the slice orientation could be influenced by the sample preparation. As both water and lipids are eliminated in the histological procedure, the histology can underestimate cartilage thickness, and cartilage morphology could be altered by histological methods, especially dehydration [29]. At 7 Tesla and a spatial resolution of $109 \times 109 \times 145\ \mu m^3$ voxel which is similar to the resolution in our study, Faure et al [30] observed a dehydration of the superficial layers of the rat knee cartilage which was not detectable with histology. According to their report, MR images obtained during the early stages of rheumatoid arthritis allowed them to study joint changes before any histological signs of attack were visible; however, cartilage quantification was not performed. At the spatial resolution of $51 \times 51 \times 94\ \mu m^3$ voxel and 7T, Goebel et al [12] reported an *in vivo* MRI-based study of healthy and OA rat knee and demonstrated the ability to assess OA-related changes in femorotibial cartilage volume/thickness in the various femorotibial compartments.

There are some limitations to this study. Firstly, this was a preliminarily exploratory study; the animal number used in the study was relatively few. The study was cross-sectional, while there was no longitudinal follow-up carried out. As discussed earlier, the MRI spatial resolution used in this study did not allow us to quantify the articular cartilage thickness or volume. Goebel et al [12] demonstrated that probably a resolution of $50 \times 50 \times 100\ \mu m^3$ voxel would be required for this. As both femoral and tibia cartilage thickness is around 180 μm [12], 50×50 μm in-place resolution would allow three to four pixels across the thickness, which is probably essential for cartilage volume or thickness assessment. In future studies, MR scans will be performed at multiple time points for follow-up of OA development, including baseline, so as to show the temporal changes. Another MR development to be explored will be ultra-short echo time (typically 20—100 μs) for cortical bone qualification [31].

In conclusion, this study showed that MRI, at the magnetic strength field of 4.7 Tesla and a spatial resolution of $59 \times 117 \times 234\ \mu m^3$, offers *in vivo* information on the changes of rat knee with OA induced using menisectomy. Compared with histology techniques, MRI allows a holistic assessment of a variety of tissues, including joint alignment, joint space widening or narrowing, meniscus, and bone and cartilage changes; thus MRI can serve as a supplement technique to histology; it is likely to be particularly useful for longitudinal follow-up of the OA model. To increase the scan time will allow further increases in spatial resolution and/or signal-to-noise ratio. However, the spatial resolution, signal-to-noise ratio, and acquisition time are mutually interdependent, therefore to optimise one of these parameters at the given magnetic field strength of 4.7 T will be at the expense of others. With the recent trend in the utilisation of higher magnetic field strengths such as 9.4 T, better quantification of small animal OA models is further expected [32,33].

Conflicts of interest

The authors have no conflicts of interest.

References

[1] Bendele AM. Animal models of osteoarthritis. J Musculoskelet Neuronal Interact 2001;1:363—76.
[2] Bendele A, McComb J, Gould T, McAbee T, Sennello G, Chlipala E, et al. Animal models of arthritis: relevance to human disease. Toxicol Pathol 1999;27:134—42.
[3] Teeple E, Jay GD, Elsaid KA, Fleming BC. Animal models of osteoarthritis: challenges of model selection and analysis. AAPS J 2013;15:438—46.
[4] Ashraf S, Mapp PI, Walsh DA. Contributions of angiogenesis to inflammation, joint damage, and pain in a rat model of osteoarthritis. Arthritis Rheum 2011;63:2700—10.
[5] Smale G, Bendele A, Horton WE. Comparison of age associated degeneration of articular cartilage in Wistar and Fischer 344 rats. Lab Anim Sci 1995;45:191—4.
[6] Janusz MJ, Bendele AM, Brown KK, Taiwo YO, Hsieh L, Heitmeyer SA. Induction of osteoarthritis in the rat by surgical tear of the meniscus: inhibition of joint damage by a matrix metalloproteinase inhibitor. Osteoarthr Cartil 2002;10:785—91.
[7] Stoop R, Buma P, van der Kraan PM, Hollander AP, Clark Billinghurst R, Robin Poole A, et al. Type II collagen degradation in articular cartilage fibrillation after anterior cruciate ligament transection in rats. Osteoarthr Cartil 2001;9:308—15.
[8] Wang YX. In vivo magnetic resonance imaging of animal models of knee osteoarthritis. Lab Anim 2008;42:246—64.
[9] Wang YX, Bradley DP, Kuribayashi H, Westwood FR. Some aspects of rat femorotibial joint microanatomy as demonstrated by high-resolution magnetic resonance imaging. Lab Anim 2006;40:288—95.
[10] Wang YX, Westwood FR. Fluid collection within the synovial sheath of the tendon of the flexor hallus longus muscle in the tarsal joint of rats: an anatomic variant detectable with magnetic resonance imaging. Lab Anim 2006;40:58—62.
[11] Wang HH, Wang YX, Griffith JF, Sun YL, Zhang G, Chan CW, et al. Pitfalls in interpreting rat knee joint magnetic resonance images and their histological correlation. Acta Radiol 2009;50:1042—8.
[12] Goebel JC, Bolbos R, Pham M, Galois L, Rengle A, Loeuille D, et al. In vivo high-resolution MRI (7T) of femoro-tibial cartilage changes in the rat anterior cruciate ligament transectionmodel of osteoarthritis: a cross-sectional study. Rheumatology (Oxford) 2010;49:1654—64.
[13] Panahifar A, Jaremko JL, Tessier AG, Lambert RG, Maksymowych WP, Fallone BG, et al. Development and reliability of a multi-modality scoring system for evaluation of disease progression in pre-clinical models of osteoarthritis: celecoxib may possess disease-modifying properties. Osteoarthr Cartil 2014;22:1639—50.
[14] Wang YX, Yan SX. Biomedical imaging in the safety evaluation of new drugs. Lab Anim 2008;42:433—41.
[15] Goebel JC, Pinzano A, Grenier D, Perrier AL, Henrionnet C, Galois L, et al. New trends in MRI of cartilage: Advances and limitations in small animal studies. Biomed Mater Eng 2010;20:189—94.
[16] Wang YX. Medical imaging in pharmaceutical clinical trials: what radiologists should know. Clin Radiol 2005;60:1051—7.
[17] Wang YX. In vivo biomedical imaging and spectroscopy in toxicogenomics and toxicoproteomics. Mol Cell Toxicol 2010;6:S28.
[18] Lee CH, Blackband SJ, Fernandez-Funez P. Visualization of synaptic domains in the Drosophila brain by magnetic

resonance microscopy at 10 micron isotropic resolution. Sci Rep 2015;5:8920.
[19] House MJ, Fleming AJ, de Jonge MD, Paterson D, Howard DL, Carpenter JP, et al. Mapping iron in human heart tissue with synchrotron x-ray fluorescence microscopy and cardiovascular magnetic resonance. J Cardiovasc Magn Reson 2014;16:80.
[20] Goebel JC, Bolbos R, Pinzano A, Schaeffer M, Rengle A, Galois L, et al. In vivo rat knee cartilage volume measurement using quantitative high resolution MRI (7 T): feasibility and reproducibility. Biomed Mater Eng 2008;18:247—52.
[21] Huang GS, Lee HS, Chou MC, Shih YY, Tsai PH, Lin MH, et al. Quantitative MR T2 measurement of articular cartilage to assess the treatment effect of intra-articular hyaluronicacid injection on experimental osteoarthritis induced by ACLX. Osteoarthr Cartil 2010;18:54—60.
[22] Lee SJ, Aadalen KJ, Malaviya P, Lorenz EP, Hayden JK, Farr J, et al. Tibiofemoral contact mechanics after serial medial meniscectomies in the human cadaveric knee. Am J Sports Med 2006;34:1334—44.
[23] Wang Y, Wluka AE, Pelletier JP, Martel-Pelletier J, Abram F, Ding C, et al. Meniscal extrusion predicts increases in subchondral bone marrow lesions and bone cysts and expansion of subchondral bone in osteoarthritic knees. Rheumatology 2010; 49:997—1004.
[24] Roos H, Lauren M, Adalberth T, Roos EM, Jonsson K, Lohmander LS. Knee osteoarthritis after meniscectomy: prevalence of radiographic changes after twenty-one years, compared with matched controls. Arthritis Rheum 1998;41: 687—93.
[25] Fernihough J, Gentry C, Malcangio M, Fox A, Rediske J, Pellas T, et al. Pain related behaviour in two models of osteoarthritis in the rat knee. Pain 2004;112:83—93.
[26] Iijima H, Aoyama T, Ito A, Tajino J, Nagai M, Zhang X, et al. Destabilization of the medial meniscus leads to subchondral bone defects and site-specific cartilage degenerationin an experimental rat model. Osteoarthr Cartil 2014;22:1036—43.
[27] Moore EE, Bendele AM, Thompson DL, Littau A, Waggie KS, Reardon B, et al. Fibroblast growth factor-18 stimulates chondrogenesis and cartilage repair in a rat model of injury-induced osteoarthritis. Osteoarthr Cartil 2005;13:623—31.
[28] Dieppe PA, Lohmander LS. Pathogenesis and management of pain in osteoarthritis. Lancet 2005;365:965—73.
[29] Cole Jr MB. Alteration of cartilage matrix morphology with histological processing. J Microsc 1984;133:129—40.
[30] Faure P, Doan BT, Beloeil JC. In-vivo high resolution three-dimensional MRI studies of rat joints at 7 T. NMR Biomed 2003;16:484—93.
[31] Chang EY, Du J, Chung CB. UTE imaging in the musculoskeletal system. J Magn Reson Imaging 2015;41:870—83.
[32] Jones MD, Tran CW, Li G, Maksymowych WP, Zernicke RF, Doschak MR. In vivo microfocal computed tomography and micro-magnetic resonance imaging evaluation of antiresorptive and antiinflammatory drugs as preventive treatments of osteoarthritis in the rat. Arthritis Rheum 2010;62: 2726—35.
[33] McErlain DD, Ulici V, Darling M, Gati JS, Vasek Pitelka V, Beier F, et al. An in vivo investigation of the initiation and progression of subchondral cysts in a rodent model of secondary osteoarthritis. Arthritis Res Ther 2012;14:R26.